U.Porto Journal of Engineering, 10:1 (2024) 1-10
ISSN 2183-6493
DOI: 10.24840/2183-6493_010-001_001279

Received: 10 January, 2023
Accepted: 19 September, 2023
Published: 30 January, 2024

# Numerical analysis of springback with experimental validation using UCB test

**Rogério F. F. Lopes**
Department of Mechanical Engineering, Faculty of Engineering, University of Porto.
Inegi, Institute of Science and Innovation in Mechanical Engineering and Industrial Engineering, Campus da FEUP, R. Dr. Roberto Frias 400, 4200-465 Porto, Portugal, (rflopes@inegi.up.pt) ORCID 0000-0002-8620-9141

**Rui L. Amaral**
Inegi, Institute of Science and Innovation in Mechanical Engineering and Industrial Engineering, Campus da FEUP, R. Dr. Roberto Frias 400, 4200-465 Porto, Portugal, (ramaral@inegi.up.pt) ORCID 0000-0002-5282-906X

**Sara S. Miranda**
Inegi, Institute of Science and Innovation in Mechanical Engineering and Industrial Engineering, Campus da FEUP, R. Dr. Roberto Frias 400, 4200-465 Porto, Portugal, (smiranda@inegi.up.pt) ORCID 0000-0002-1016-280X

**Abel D. Santos**
Department of Mechanical Engineering, Faculty of Engineering, University of Porto, (abel@fe.up.pt) ORCID 0000-0003-1345-651X

**Pedro M. G. P. Moreira**
Inegi, Institute of Science and Innovation in Mechanical Engineering and Industrial Engineering, Campus da FEUP, R. Dr. Roberto Frias 400, 4200-465 Porto, Portugal, (pmoreia@inegi.up.pt) ORCID 0000-0002-1127-2525

**Author Keywords**

**Automotive Industry, Springback, Sheet Metal Forming, FEM.**

**Type: Research Article**

Open Access
Peer Reviewed


**Abstract**

Sheet metal forming is used to process a substantial percentage of automobile components, and the so-called springback behavior is of primary importance, in order to obtain the final part with an accurate geometry. This paper describes a springback research that employs three different materials often used in the automobile industry: DP780, HSLA420, and AA5754. The unconstrained cylindrical bending test (UCB test) will be utilized to assess the springback prediction for selected materials. In this study, experimental data is collected and numerical results are provided utilizing finite element techniques.
Results show that UCB test is an adequate benchmark for analysis of springback behavior of sheet metallic materials and it has also been observed a close agreement between numerical results and experiments.

## 1. Introduction

Safety requirements and low fuel consumptions are current challenges for the automobile industry, which require newer materials and solutions in sheet metal forming (Amaral et al. 2020). The impact of springback is one of the most prevalent flaws in this manufacturing process, since it influences directly the final geometry of the component, compromising the precision of the final product and its quality (Jing et al. 2021, Cinar et al. 2021). Due to residual stresses upon unloading, the part relaxes tending to achieve the static equilibrium (Tisza and Lukacs 2014, Wagoner, Lim, and Lee 2013, Amaral et al. 2020, Rodrigues 2015). Figure 1.a) depicts a metallic sheet that has been bent, which shows a geometric change induced by elastic behavior after the tools are removed (Lopes 2019). This geometric change, known as springback, is critical since it creates difficulties to meet the dimensional specifications to

produce parts. This fault is caused mostly by reasons such as: *(i)* an excessive bending radius/thickness ratio, *(ii)* mechanical properties of the materials, and *(iii)* process parameters such as blankholder pressure or lubrication (Barata da Rocha and Ferreira Duarte 2005, Lopes 2019).


a) b)

**Figure 1:** a) Sheet bending springback effect and b) Springback angle definition

To mitigate this impact, several conventional approaches based on trial-and-error are still in use. However, this is costly in resources and time, while nowadays numerical procedures may be applied to predict and compensate the elastic recovery of component after tool removal (Chongthairungruang et al. 2013).

The UCB (unconstrained cylindrical bending) test is a benchmark, which was proposed by Numisheet conference series for assessment of springback (Lee et al. 2009, Gou et al. 2020) and it is chosen in this research to evaluate the behavior for proposed materials, since it involves a simple geometry while promoting high elastic recovery for the metallic sheet and includes contact with friction, thus evaluating also the numerical approach and accuracy of the finite element analysis (Lee et al. 2009, Gou et al. 2020). The geometry of the tools is predefined and depicted in the Figure 2.

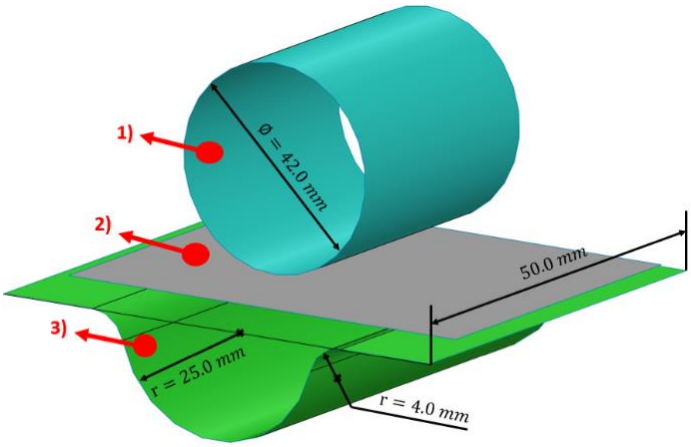


**Figure 2:** Geometry and dimensions of the UCB test tools: 1) Punch, 2) Sheet and 3) Die

The procedure is divided into two stages: The first stage corresponds to moving the punch down, the blank being bended up to a clearance of 0.5 mm with the die and the second step corresponds to moving the punch up, thus releasing the specimen and being defined the final geometry after springback (Lopes 2019). Then, the springback can be measured by comparing the angle before and after removing the tools, as shown in the Figure 1.b). Many investigations of springback utilizing the UCB test may be found in the literature (Alves de Sousa et al. 2008, Ahn et al. 2009, Alves, Oliveira, and Menezes 2004). In this research the study uses different sheet materials of current industrial interest by combining not only numerical procedures but also experimental validation.

## 2. Materials and Methods

The selected three different materials are the following: DP780 steel and HSLA420 steel, as well as the aluminum alloy AA5754. The fundamental material properties and thicknesses are shown in Figure 3.b) (Lopes 2019, Pimentel 2018) and the hardening behavior is presented in the Figure 3.a). Each material has a different hardening equation, which best fits to its behavior, DP780 uses Swift-Voce equation (Zhang et al. 2021), HSLA420 uses Swift and AA5754 uses Voce equation, as defined by Equations (1) to (3) and corresponding parameters are displayed in the Table 1.

$$\textit{DP780:} \quad \sigma = \alpha \cdot [K \cdot (\varepsilon_0 + \varepsilon)^n + (1-\alpha) \cdot [A + B \cdot (1 - e^{-C\varepsilon})] \tag{1}$$

$$\textit{HSLA420:} \quad \sigma = K \cdot (\varepsilon_0 + \varepsilon)^n \tag{2}$$

$$\textit{AA5754:} \quad \sigma = A + B \cdot (1 - e^{-C\varepsilon}) \tag{3}$$

| Material | $\alpha$ | $K$ | $\varepsilon_0$ | $n$ | A [MPA] | B [MPA] | C |
|---|---|---|---|---|---|---|---|
| **DP780** | 0.661 | 1834.1 | 0.0025 | 0.0892 | -551.4 | 405.26 | 31.31 |
| **HSLA420** | - | 930 | 0.023 | 0.118 | - | - | - |
| **AA5754** | - | - | - | - | 121.95 | 132.05 | 17.46 |

**Table 1:** Parameters of the hardening curves for the studied materials

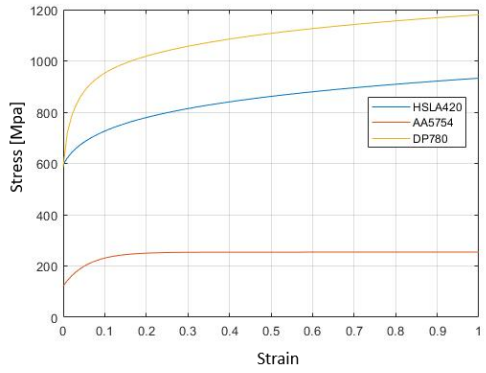


a)

| Material / Properties | DP780 | HSLA420 | AA5754 |
|---|---|---|---|
| Young Modulus [GPa] | 210 | 210 | 70 |
| Poisson Coefficient, $\nu$ | 0.3 | 0.3 | 0.33 |
| Density, $\rho$ $[kg/m^3]$ | 7800 | 7800 | 2700 |
| Yield Strength, $R_{p0.2}$ $[MPa]$ | 526 | 432 | 121.6 |
| Ultimate Strength, Rm [MPa] | 843 | 488 | 231.8 |
| Thickness, t [mm] | 0.8 | 1.5 | 1 |

b)

**Figure 3:** a) Hardening curves of the testing materials and) mechanical properties and thickness of the materials

The finite element code PamStamp (group 2021) will be used for the numerical part of this study. Regarding the used formulation, only *Belytschko-Tsay* element type will be used (Lopes 2019).

In terms of boundary conditions, the die is fixed, while the punch is the moving tool. The punch goes down with a defined displacement up to depth that leaves a clearance of 0.5 mm between sheet and die. The analysis is explicitly formulated during the deformation process by activation of the ramp command, which smooths accelerations and minimizes inertial effects. On the other hand, the springback simulation is modelled with an implicit solver, thus allowing a more efficient and accurate analysis of releasing the residual stresses after bending.

Regarding the outputs, there are 10 steps divided evenly, according to the defined displacement of the punch. The final step of springback is performed by removing tools, the corresponding forces for contacting nodes are considered and an implicit analysis is done until final equilibrium of the part is reached and final geometry is obtained. Figure 4 depicts the stamping process for the defined steps in this bending process.

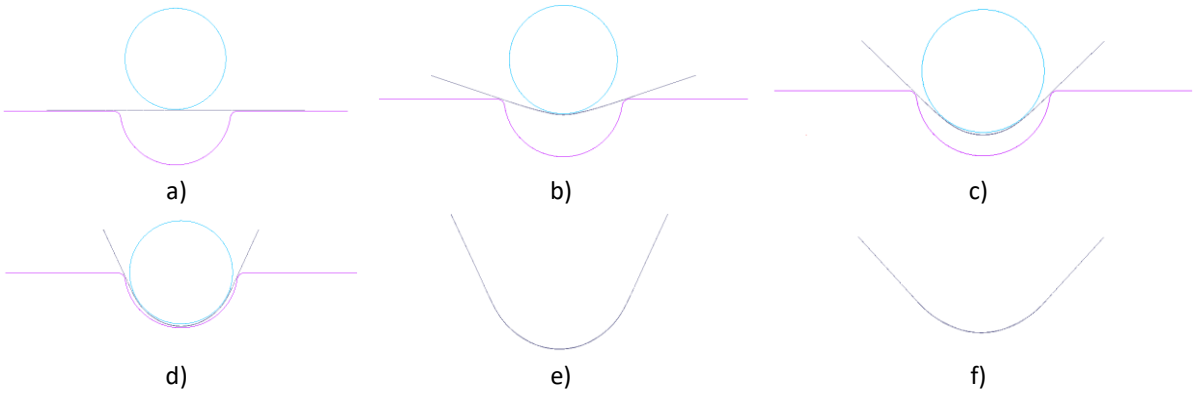


**Figure 4:** Stamping process: a) Step 0, b) Step 4, c) Step 8, d) Final stage, e) Step 0, before springback and f) final step, after springback

## 3. Results and Discussion

### *3.1. Sensitivity analysis of the numerical parameters*

Some numerical variables shall be defined to optimize the numerical model, in order to determine the best balance, such as the definition of mesh size and punch velocity having also in mind the corresponding computational cost.

At first, we are investigating the effect of the mesh size. This numerical sensitivity analysis will only be undertaken for one material, being selected the DP780 steel. The PamStamp code has the capability of automatic refining mesh throughout the workflows after specifying the initial mesh size. As a result, the final values are already optimized. In terms of mesh size, the study will initially be conducted for the cases of $10 \times 10\ mm$, $8 \times 8\ mm$, $4 \times 4\ mm$, and $2 \times 2\ mm$. Furthermore, the velocity of the impactor is being investigated for $5\ m/s$, $1 m/s$, $0.5 m/s$, $0.1 m/s$ and $0.05\ m/s$ in order to determine its influence on simulation results.

The tools are defined as rigid and their discretization is performed when the geometries are imported. In terms of tools, the punch has 884 elements while the die has 1360.

The simulation code is being used with adaptive refinement techniques which will adapt the discretization and mesh size to local needs for deformation or contact, especially in small radius.

Considering the situation when the mesh is defined an element size of $10 \times 10\ mm$, blank is discretized by 36 elements at the start of the modeling process, but the zones with higher contact with punch and die radius are refined, thus totaling 774 elements at the end of simulation, as shown in the Figure 5.

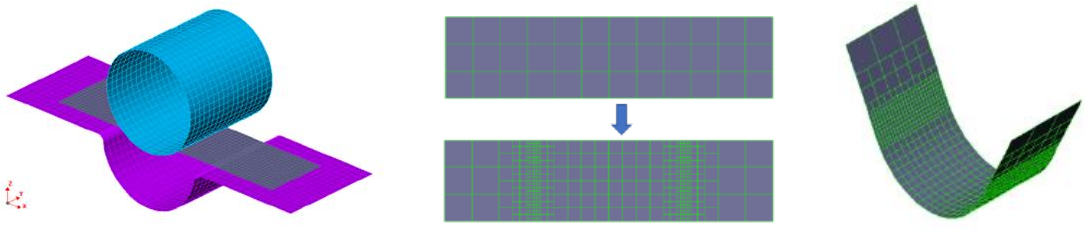


**Figure 5:** a) UCB FE model, b) Remeshing process during the loading and c) Final mesh of the sheet

Table 2 summarizes the computation time for various meshes and velocities as the number of elements changes. Because the total time for analysis is acceptable, even for the smallest

element size, the mesh size was maintained at 2x2 mm to study the sensitivity of velocity variable.

| Mesh | CPU time [min] | Number of elements | | |
|---|---|---|---|---|
| | | On modelling | State 0 | Final State |
| 10x10 | 0:51 | 36 | 360 | 774 |
| 8x8 | 1:20 | 60 | 432 | 1068 |
| 4x4 | 1:30 | 240 | 528 | 1176 |
| 2x2 | 2:30 | 900 | 1080 | 1440 |

a)

| Velocity [m/s] | CPU time [min] |
|---|---|
| 5 | 0:35 |
| 1 | 1:30 |
| 0.5 | 2:40 |
| 0.1 | 11:11 |
| 0.05 | 21:56 |

b)

**Table 2:** Computation times and number of elements for each mesh and b) computation times for each speed

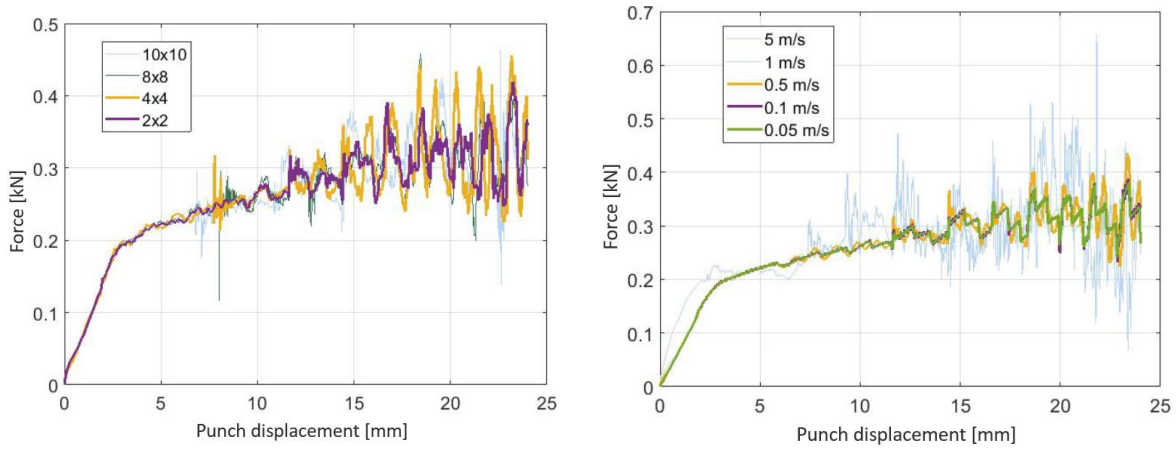


a) b)

**Figure 6:** Force/displacement of the punch for different mesh sizes and b) Force/displacement of the punch for different velocities

The impact of mesh size and velocity on results for force-displacement curve are depicted in Figure 6. Results show that the discretization of the mesh has minimal effect on the behavior of the obtained curves. Nevertheless, when the force surpasses a particular value, the biggest oscillations for bigger mesh sizes are decreased by a smaller mesh size. As the number of elements increases, the number of contact points increase, thus making the impact of oscillations less noticeable.

Regarding the effect of velocity, it is worth noting the obvious noise at greater speeds, when the dramatic inertial effects are more visible. Velocity of $5\ m/s$ it is clearly the most critical case among the chosen speeds. For the lower speeds, the values tend to acquire a more uniform evolution leading to the decreasing of oscillations. It is seen that computation time increases significantly for speed lower than $0.1\ m/s$, as presented in the Table 2.

According to the results for sensitivity analysis, the numerical model was defined by selecting the finer mesh size of 2x2 mm and the best balance for punch velocity was considered as 0.5 m/s.

### *3.2. Experimental Results and Validation*

In this study a universal testing machine was used. This machine can perform experimental tests, namely tensile tests, compression and bending tests, being possible the output of displacement data and the force applied to the specimens. An experimental tool has been manufactured and adapted to the universal machine, according to dimensions defined in

Figure 2 and specification of UCB benchmark. Experimental bending tests are performed for selected materials, DP780, HSLA40 and AA5754.

### *3.2.1. DP780*

The specimen dimensions of this material is 120x30x0.8 mm and the punch moves $24\ mm$ down. The force/displacement plot is represented in Figure 7.a) which shows the experimental curve (red) compared to the numerical one (blue). As seen there is a good correlation between the values obtained experimentally and the evolution of the numerical simulation. The corresponding sheet geometry, before and after springback, for numerical results is presented in the Figure 7.b). The post-processing capabilities for Pam-Stamp code allows to measure the angle between two vectors and therefore to know the springback angle.

Regarding to the experimental values of the angles, they are presented in the Figure 8, before and after springback. By measuring these angles, the comparison with the numerical values is quantified in the Table 3. For this material the relative deviation is $15.27\%$.

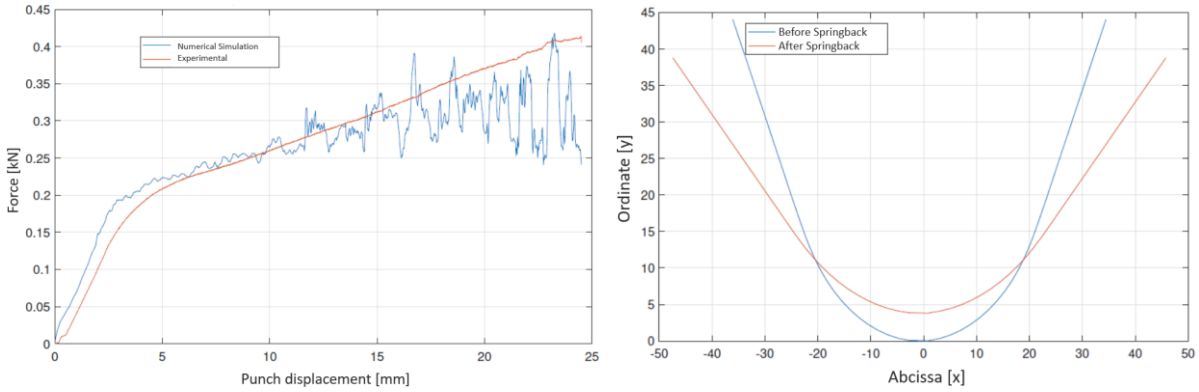


a) b)

**Figure 7:** DP780 steel a) Force /Displacement for experimental and numerical results and b) Sheet geometry, before and after springback, for numerical results.

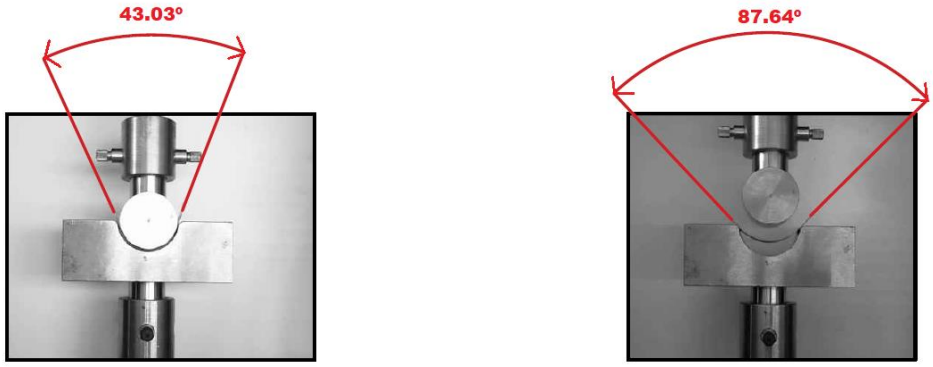


a) b)

**Figure 8:** Experimental measured angle for DP780: a) Before springback and b) after springback.

| Result | $\boldsymbol{\theta_f}$ | $\boldsymbol{\theta_s}$ | $\Delta\boldsymbol{\theta}$ | $relative\ deviation\ (\%)$ |
|---|---|---|---|---|
| Experimental | $43.03°$ | $87.64°$ | $44.61°$ | $\frac{\Delta\boldsymbol{\theta}_{Exp} - \Delta\boldsymbol{\theta}_{FEM}}{\Delta\boldsymbol{\theta}_{FEM}} = \frac{44.61° - 38.70°}{38.70°} \times 100\% = 15.27\%$ |
| FEA | $44.96°$ | $83.66°$ | $38.70°$ | |

**Table 3:** Synthesis of the obtained angles via experimental vs. numerical, its relative deviation calculation for DP780 material.

### *3.2.2. HSLA420*

The specimen dimensions of this material are 120x10x1.5 mm and the punch moves $23.5\ mm$ down. As this material is $1.5\ mm$ thick, it was necessary to reduce the total punch displacement in order to get a clearance of 0.5 mm to the die. On the other hand, since the experimental load cell is limited to $0.5\ kN$ and the predicted force by FEA would exceed this limit it was necessary to reduce the width of the specimen from 30 mm to 10 mm.

Figure 9.a) shows the force/displacement plot for experimental and numerical results, while Figure 9.b) presents the numerical sheet profile, before and after springback. Figure 10 denotes the experimental setup and corresponding angles, before and after springback. The relative deviation of this material is $2.85\%$, as shown in the Table 4.

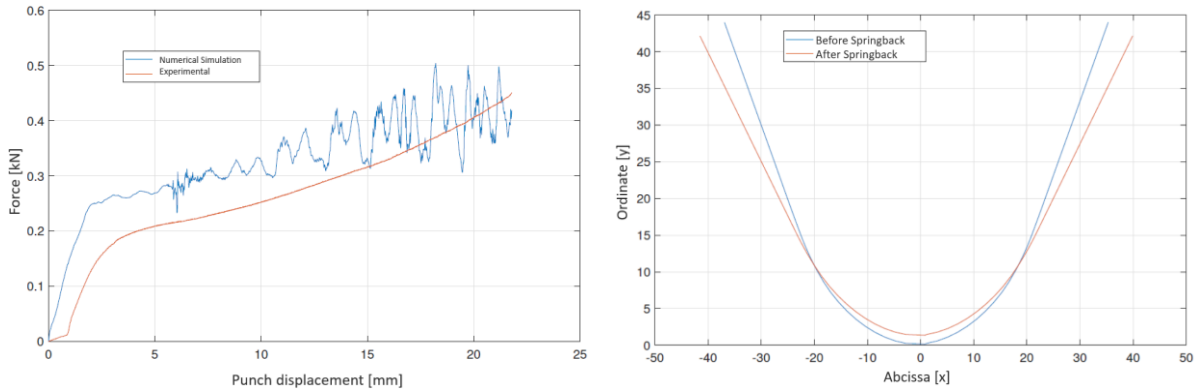


a) b)

**Figure 9:** HSLA420 steel a) Force /Displacement for experimental and numerical results and b) Sheet geometry, before and after springback, for numerical model.

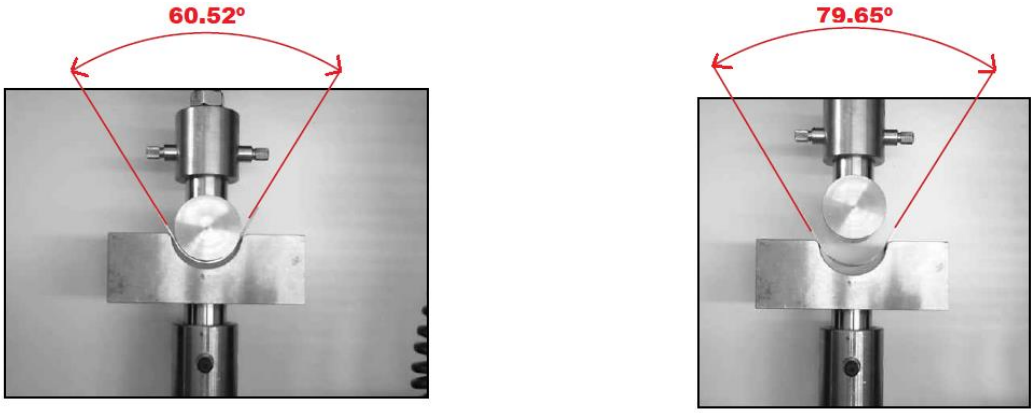


a) b)

**Figure 10:** Experimental measured angle for HSLA420: a) Before springback and b) after springback.

| Result | $\boldsymbol{\theta_f}$ | $\boldsymbol{\theta_s}$ | $\Delta\boldsymbol{\theta}$ | $relative\ deviation\ (\%)$ |
|---|---|---|---|---|
| Experimental | 60.52° | 79.65° | 19.13° | $\frac{\Delta\boldsymbol{\theta}_{Exp} - \Delta\boldsymbol{\theta}_{FEM}}{\Delta\boldsymbol{\theta}_{FEM}} = \frac{19.13° - 18.60°}{18.60°} \times 100\% = 2.85\%$ |
| FEA | 62.80° | 81.40° | 18.60° | |

**Table 4:** Synthesis of the obtained angles via experimental vs. numerical, its relative deviation calculation for HSLA420 material.

### *3.2.3. AA5754*

The specimen dimensions of this material are 120x80x1 mm, which is identical to what was done previously. Figure 11.a) shows the force/displacement plot for experimental and

numerical results. It is seen that the noise occurs earlier than in other materials, as previously stated. Also, it is observed that level of force seen here is significantly lower than that observed in previous materials. Table 5 shows the springback experimental vs. numerical results, which indicate a low relative difference of 6.24%.

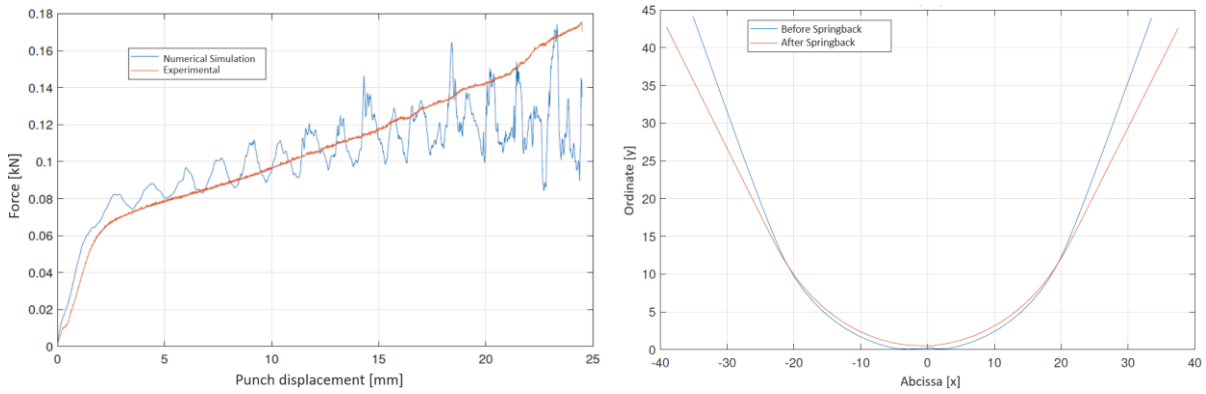


a) b)

**Figure 11:** Aluminum alloy AA5754 a) Force /Displacement for experimental and numerical results and b) Sheet geometry before and after springback, for numerical model.


a) b)

**Figure 12:** Experimental measured angle for AA5754: a) Before springback and b) after springback.

| Result | $\boldsymbol{\theta_f}$ | $\boldsymbol{\theta_s}$ | $\Delta\boldsymbol{\theta}$ | $relative\ deviation\ (\%)$ |
|---|---|---|---|---|
| Experimental | 38.90° | 60.00° | 21.10° | $\frac{\Delta\boldsymbol{\theta}_{Exp} - \Delta\boldsymbol{\theta}_{FEM}}{\Delta\boldsymbol{\theta}_{FEM}} = \frac{21.10° - 19.86°}{19.86°} \times 100\% = 6.24\%$ |
| FEA | 44.25° | 64.11° | 19.86° | |

**Table 5:** Synthesis of the obtained angles via experimental and FEM its relative deviation calculation for AA5754 material.

### *3.3. Discussion of the results*

Regarding the force/displacement of the punch, there is a suitable accordance between FEA and experimental data. However, there is some noise in the FEM component, which is due to being an explicit analysis and inertial effects can take some effects. As seen in the sensitivity analysis this noise can be minimized by slowing down the punch velocity, but a good balance with computational cost has been kept for the model. In terms of springback prediction and the validation with experiments, the difference between experimental and numerical values is relatively low in the case of HSLA420 and AA5754, confirming the good accuracy of the model, 2.85% and 6.24%, respectively. In case of DP780 steel, the difference increases slightly to 15.27%, but it should be highlighted that this material, being a higher strength

material it has a much higher springback, which may give rise to higher needed accuracy for mechanical characterization for its hardening behavior and the possibility of nonlinear elastic unloading-reloading behavior.

## 4. Conclusions

The springback behavior of three different sheet metallic materials were studied using finite element Pam-Stamp code and experiments were performed, in order to validate numerical results. These materials are most commonly used in the automobile industry and they correspond to DP780 steel, HSLA420 steel and the aluminum alloy AA5754).

The quantity of manufactured components of these materials employing sheet metal forming process is significant high. As a result, it is critical to strive to reduce the defects associated of this manufacturing process, being springback one of the most significant variables affecting the final geometry of a sheet metal component. In order to quantify the springback, the so-called unconstrained cylindrical bending test (UCB test) is used. In this test the springback is measured by the angle difference between the instant before and after the punch release. This analysis considers a comparison between the experimental results and those predicted by FEA. Experimental tests were collected using a universal testing machine, which allowed to acquire the force/displacement evolution, as well as the profile geometry needed to validate numerical predicted results.

An initial step for creating the FE model it was to investigate the mesh sensitivity and punch velocity influence. The selected values for initial mesh size were 2x2 mm and for punch velocity was 0.5 mm/s, which corresponded to a best balance between accuracy and computational cost.

With regard to springback predicted results, there is a good agreement between the springback angle of the FE model and the experimental results, in the case of HSLA420 and AA5754. A higher difference observed in DP780 steel suggests that further investigation should be done with a direction on its mechanical characterization for hardening and elastic behavior.

## Acknowledgments

The authors gratefully acknowledge the financial support of the Portuguese Foundation for Science and Technology (FCT) under the projects POCI-01-0145-FEDER-030592, POCI-01-0145-FEDER-031243 and NORTE-01-0145-FEDER-032419 by UE/FEDER through the programs COMPETE 2020 and FEDER. The third author is also grateful to the FCT for the Doctoral grant SFRH/BD/146083/2019 under the program POCH, co-financed by the European Social Fund (FSE) and Portuguese National Funds from MCTES.

## References

Ahn, Kanghwan, Donghoon Yoo, Min Hong Seo, Sung-Ho Park, and Kwansoo Chung. 2009. "Springback prediction of TWIP automotive sheets." *Metals and Materials International* 15 (4):637-647. doi: https://doi.org/10.1007/s12540-009-0637-z.

Alves de Sousa, R. J., J. P. M. Correia, F. J. P. Simões, J. A. F. Ferreira, R. P. R. Cardoso, J. J. Gracio, and F. Barlat. 2008. "Unconstrained springback behavior of Al–Mg–Si sheets for different sitting times." *International Journal of Mechanical Sciences* 50 (9):1381-1389. doi: https://doi.org/10.1016/j.ijmecsci.2008.07.008.

Alves, J. Luís, Marta Oliveira, and Luís Filipe Menezes. 2004. "Springback Evaluation with Several Phenomenological Yield Criteria." *Materials Science Forum* 455-456:732-736. doi: https://doi.org/10.4028/www.scientific.net/MSF.455-456.732.

Amaral, Rui L., Diogo M. Neto, Dipak Wagre, Abel D. Santos, and Marta C. Oliveira. 2020. "Issues on the Correlation between Experimental and Numerical Results in Sheet Metal Forming Benchmarks." *Metals* 10 (12). doi: https://doi.org/10.3390/met10121595.

Barata da Rocha, A., and J. Ferreira Duarte. 2005. *Tecnologia da Embutidura*.

Chongthairungruang, B., V. Uthaisangsuk, S. Suranuntchai, and S. Jirathearanat. 2013. "Springback prediction in sheet metal forming of high strength steels." *Materials & Design* 50:253-266. doi: https://doi.org/10.1016/j.matdes.2013.02.060.

Cinar, Zeki, Mohammed Asmael, Qasim Zeeshan, and Babak %J Jurnal Kejuruteraan Safaei. 2021. "Effect of springback on A6061 sheet metal bending: a review." 33 (1):13-26.

Gou, Rui-bin, Wen-jiao Dan, Wei-gang Zhang, and YU %J Materials Science Min. 2020. "Prediction on the Mechanical and Forming Behaviors of Ferrite-Martensite Dual Phase Steels Based on a Flow Model." 26 (4):401-407.

group, ESI. 2021. "Stamping & Forming Simulation Software." *Available online: https://www.esi-group.com/products/sheet-metal-forming (accessed on December 2021)*.

Jing, Zhou, Yang Xiaoming, Wang Baoyu, and Xiao Wenchao. 2021. *The International Journal of Advanced Manufacturing Technology*. doi: Https://doi.org/10.21203/rs.3.rs-322846/v1.

Lee, M. G., S. J. Kim, R. H. Wagoner, K. Chung, and H. Y. Kim. 2009. "Constitutive modeling for anisotropic/asymmetric hardening behavior of magnesium alloy sheets: Application to sheet springback." *International Journal of Plasticity* 25 (1):70-104. doi: https://doi.org/10.1016/j.ijplas.2007.12.003.

Lopes, Rogério Filipe Ferreira. 2019. "Simulação Numérica e Validação Experimental de Benchmarks, Aplicados na Conformação Plástica de Chapas." *Dissertação de Mestrado, Faculdade de Engenharia, Universidade do Porto.* https://hdl.handle.net/10216/122411.

Pimentel, Anthony Michael Fernandes. 2018. "Caracterização experimental e modelação numérica do comportamento mecânico de chapas multi-camada e multi-material: aplicação à indústria automóvel." *Tese de Doutoramento em Engenharia Mecânica, Universidade do Minho.* http://hdl.handle.net/1822/60061.

Rodrigues, Bárbara Rita Teixeira. 2015. "Revisão do processo de embutidura para melhoria da calibração de componentes no processo de soldadura Laser Amtrol-Alfa." *Dissertação de Mestrado, Faculdade de Engenharia, Universidade do Porto.* https://repositorio-aberto.up.pt/handle/10216/89904.

Tisza, Miklós, and Zsolt Lukacs. 2014. "Springback Analysis of High Strength Dual-phase Steels." *Procedia Engineering* 81. doi: https://doi.org/10.1016/j.proeng.2014.10.127.

Wagoner, Robert H., Hojun Lim, and Myoung-Gyu Lee. 2013. "Advanced Issues in springback." *International Journal of Plasticity* 45:3-20. doi: https://doi.org/10.1016/j.ijplas.2012.08.006.

Zhang, Chong, Yanshan Lou, Saijun Zhang, Till Clausmeyer, A. Erman Tekkaya, Lei Fu, Qiang Chen, and Qi Zhang. 2021. "Large strain flow curve identification for sheet metals under complex stress states." *Mechanics of Materials* 161:103997. doi: https://doi.org/10.1016/j.mechmat.2021.103997.